J Nanopart Res (2014) 16:2627
DOI 10.1007/s11051-014-2627-4

RESEARCH PAPER

Solid-stabilized emulsion formation using stearoyl lactylate coated iron oxide nanoparticles

Pranav S. Vengsarkar · Christopher B. Roberts

Received: 6 July 2014 / Accepted: 26 August 2014 / Published online: 7 September 2014

Abstract Iron oxide nanoparticles can exhibit highly tunable physicochemical properties that are extremely important in applications such as catalysis, biomedicine and environmental remediation. The small size of iron oxide nanoparticles can be used to stabilize oil-in-water Pickering emulsions due to their high energy of adsorption at the interface of oil droplets in water. The objective of this work is to investigate the effect of the primary particle characteristics and stabilizing agent chemistry on the stability of oil-in-water Pickering emulsions. Iron oxide nanoparticles were synthesized by the co-precipitation method using stoichiometric amounts of Fe^{2+} and Fe^{3+} salts. Sodium stearoyl lactylate (SSL), a Food and Drug Administration approved food additive, was used to functionalize the iron oxide nanoparticles. SSL is useful in the generation of fat-in-water emulsions due to its high hydrophilic–lipophilic balance and its bilayer-forming capacity. Generation of a monolayer or a bilayer coating on the nanoparticles was controlled through systematic changes in reagent concentrations. The coated particles were then characterized using various analytical techniques to determine their size, their crystal structure and surface functionalization. The capacity of these bilayer coated nanoparticles to stabilize oil-in-water emulsions under various salt concentrations and pH values was also systematically determined using various characterization techniques. This study successfully demonstrated the ability to synthesize iron oxide nanoparticles (20–40 nm) coated with SSL in order to generate stable Pickering emulsions that were pH-responsive and resistant to significant destabilization in a saline environment, thereby lending themselves to applications in advanced oil spill recovery and remediation.

Keywords Iron oxide nanoparticles · Sodium stearoyl lactylate · Co-precipitation · Pickering emulsions

Introduction

Iron oxide nanoparticles are an integral part of contemporary nanoparticle research due to their unique physicochemical properties and wide applicability. These applications include their use as magnetic resonance imaging (MRI) contrast agents (Andreas et al. 2012; Babes et al. 1999; Hong et al. 2008; Hu et al. 2011; Kwak 2005; Qiao et al. 2009), drug delivery agents (Avdeev et al. 2010; Jain et al. 2005; Morales et al. 2005, 2008), catalysts (Hosseinian et al. 2011; Khedr et al. 2009; Park et al. 2010; Torres

Electronic supplementary material The online version of this article (doi:10.1007/s11051-014-2627-4) contains supplementary material, which is available to authorized users.

P. S. Vengsarkar · C. B. Roberts (✉)
Department of Chemical Engineering, Auburn University, 212 Ross Hall, Auburn, AL 36849-5127, USA
e-mail: croberts@eng.auburn.edu

Galvis et al. 2012), and for the formation of Pickering emulsions (Binks and Whitby 2005; Zhou et al. 2012). The ability to produce monodisperse nanoparticles that are dispersible in various solvents (aqueous and organic) is necessary for their use in the applications listed above. In addition to this, the interfacial properties of the iron oxide nanoparticles can be tuned, using different stabilizing ligands, to ensure the applicability of the nanoparticles in their respective applications. The interfacial properties of the iron oxide nanoparticles are especially critical in applications which involve surface based phenomena like catalysis, micro-electro-mechanical devices and emulsion stabilization.

In an emulsion, droplets of one liquid are dispersed in another immiscible liquid, and these droplets are usually stabilized by an emulsifier. An emulsifier is a molecule (usually a surface active amphiphile) which adsorbs at the oil–water interface and forms a protective film to resist droplet coalescence and phase separation (Qiao et al. 2012). In 1907, Pickering observed that colloidal particles which were located at the oil–water interface can also be used to stabilize emulsions of oil and water (Melle et al. 2005). These Pickering emulsions have remarkable stability due, in part, to the extremely high energies of attachment for particles held at liquid–liquid interfaces (Binks and Lumsdon 2001). Previous studies have shown that extremely effective Pickering emulsions can be formed using nanoparticles of various materials like latex, (Binks and Lumsdon 2001) carbonyl iron, (Melle et al. 2005) fatty acid-coated iron oxide, (Ingram et al. 2010; Lan et al. 2007) silica, (Binks and Whitby 2005; He and Yu 2007) titanium dioxide, (Chen et al. 2007) and zinc oxide (Chen et al. 2010). Pickering emulsions have various applications especially in the biomedical field where they have been investigated in the controlled release of drugs like ibuprofen.(Zhang et al. 2009) They also have various applications in areas like heavy oil transportation, oil recovery and emulsion polymerization. (Li and Stöver 2008) Pickering emulsions generated through the use of nanoparticles are also being investigated for use as alternative or supplementary dispersants for oil-spill remediation applications. (Katepalli et al. 2013; Saha et al. 2013; Sullivan and Kilpatrick 2002) Magnetic nanoparticles can also be used to form these Pickering emulsions, which add magnetism as another controlling factor to tune the emulsion forming capacity of the particles and the stability of the generated emulsions (Brown et al. 2012; Melle et al. 2005; Orbell et al. 1997, 2007). Lan et al.(2007) and Ingram et al.(2010) have shown through previous studies that surface-modified iron oxide nanoparticles at low concentrations (1 and 0.14 %, respectively) are capable of stabilizing oil-in-water Pickering emulsions. The particles used in both these studies were coated with oleic acid, which is a popular stabilizing ligand for iron oxide nanoparticles (Wang et al. 2010; Zhang et al. 2006). Zhou et al. (2012) and Qiao et al. (2012) have also reported the stabilization of Pickering emulsions using iron oxide nanoparticles coated with silane coupling agents and a variety of carboxylic acids.

The aim of this particular study is to controllably synthesize magnetic iron oxide nanoparticles coated with a relatively benign stabilizing ligand (i.e., sodium stearoyl lactylate) and to test the pH and salinity responsiveness of Pickering emulsions generated through the use of these particles. Sodium stearoyl lactylate (SSL) is a biodegradable, FDA approved, food-additive which is primarily used as a dough-strengthener and processing aid in baked products (European Food Safety Authority 2013; Flores et al. 2007; Lamb et al. 2010) and toxicity studies on SSL using rats have shown no statistically significant health effects (Lamb et al. 2010). Industrial grade SSL is manufactured through the esterification of commercial grade lactic and stearic acid, followed by neutralization. It should be noted that since lactic acid contains a hydroxyl as well as a carboxyl group, the stearic acid can be esterified to a single lactic acid or lactic acid polymer in commercially available SSL. This results into the presence of multiple species of lactylate esters (e.g., stearoyl-2-lactylate, stearoyl-3-lactylate), along with unreacted lactic acid in commercially available SSL. (Whitehurst 2008) The high emulsifying efficiency of SSL is countered by the fact that it is poorly soluble in aqueous and organic solutions,(Grigoriev et al. 2007) which reduces its applicability outside the food industry. SSL is an anionic emulsifier and is useful in the generation of oil-in-water (O/W) emulsions due to its high hydrophilic–lipophilic balance and excellent bilayer-forming capacity. (Kokelaar et al. 1995; Kurukji et al. 2013) The capacity of SSL to stabilize emulsions is based on the amphiphilic nature of the SSL molecule, consisting of a hydrophilic charged head and a long hydrophobic hydrocarbon tail. (Sovilj et al. 2013) The

presence of multiple carbonyl functionalities also gives a chance for one or two of the carbonyl groups to coordinate with the metal oxide surface. (Lodhia et al. 2010) Previous studies have shown that SSL, by itself, can be used as an emulsifier for O/W emulsions,(Kurukji et al. 2013) or it can be used with other surface active agents like chitosan (Zinoviadou et al. 2011) or carrageenan (Flores et al. 2007) to give emulsions with increased stability to coalescence and creaming.

In this study, by carefully varying the amount of SSL added to the reaction system, it was aimed to controllably synthesize monolayer and bilayer coated iron oxide nanoparticles. After analyzing these particles using various particle characterization methods to determine the surface functionalization of the iron oxide core, these surface-modified particles were then investigated for their capacity to stabilize oil-in-water Pickering emulsions. The generated Pickering emulsions were also tested for their pH and salinity responsiveness so as to assess the stability and practical applicability of the emulsions.

Experimental section

Materials

Iron (III) chloride hexahydrate ($FeCl_3 \cdot 6H_2O$, 99.9 %), iron (II) chloride tetrahydrate ($FeCl_2 \cdot 4H_2O$, 99.9 %), hydrochloric acid (HCl, 36 wt% aq. soln.), tetramethylammonium hydroxide (TMAOH, 1.0 M solution, ACS grade), *n*-dodecane (99+ %) and *n*-hexane (HPLC grade, 95 %), were obtained from Alfa Aesar, USA. Ammonium hydroxide (5 N, reagent grade) was obtained from BDH Chemicals, USA and sodium stearoyl lactylate (SSL) (acid value 60–80) was obtained from Spectrum Chemicals, USA. Acid Blue 9 ($C_{37}H_{34}N_2Na_2O_9S_3$) water soluble dye was obtained from TCI America. All chemicals were used as received without further purification.

Iron oxide nanoparticle synthesis

Iron oxide nanoparticles coated with sodium stearoyl lactylate were synthesized using a technique based upon the coprecipitation method described previously by Jain et al. (2005). In this method Fe(III) and Fe(II) salts are mixed in stoichiometric amounts in a basic solution to yield iron oxide nanoparticles. Initially aqueous solutions of 0.1 M Fe(III) and 0.1 M Fe(II) were prepared using DIUF water and the iron chloride salts. 30 mL of Fe(III) solution was mixed with 15 mL of Fe(II) solution in a three-necked flask with vigorous magnetic stirring. Under constant stirring and under a nitrogen atmosphere, 3 mL of 5 M ammonium hydroxide was added to this mixture to generate a black precipitate of iron oxide nanoparticles. The temperature of this system was then increased to 80 °C and maintained for 30 min to evaporate the ammonia out of the solution. While the temperature was being increased, a predetermined amount of SSL (powder) (25–800 mg) was added to the mixture. The SSL powder was added slowly, under constant stirring to ensure complete dissolution. The system temperature was then lowered to 60 °C and held there for 1 h. The system was then allowed to cool down to room temperature. Depending upon the amount of SSL used during synthesis, the nanoparticles either precipitated out of the aqueous solution or remained dispersed in the water post-synthesis. Since the sodium counter-ion in SSL will be present in solution and not attached to the particles, the particles will be henceforth referred to as stearoyl lactylate (SL) coated iron oxide nanoparticles. For the particles which precipitated out of the aqueous solution, separation using magnetic decantation was carried out followed by washing with DIUF water and dispersal in an organic solvent (hexane/dodecane). For the particles which remained dispersed in the aqueous solution, purification of the particles was performed by first dialyzing 10 mL batches of the solution using multiple disposable dialyzers (Spectrum Labs Float-A-Lyzer® G2) for 12 h in DIUF water. The solution obtained post dialysis was then centrifuged in 10 mL batches with a Pall Macrosep® Advance Centrifugal device to remove any salt impurities. During these purification steps, DIUF water was added where necessary to recover the particles from the membrane surfaces.

Characterization of SL coated iron oxide nanoparticles

The core size and size distribution of the synthesized nanoparticles was determined through the use of transmission electron microscopy (TEM). Carbon-coated TEM grids of the nanoparticles (obtained post-purification) were then prepared via dropcasting and micrographs were acquired on a Zeiss EM 10

transmission electron microscope. The images obtained from the TEM were sized using the ImageJ software package. Hydrodynamic diameter of the coated particles was also measured through the use of dynamic light scattering (DLS) using a NICOMP^{TM} 380 Submicron Particle Sizer. The stability of the particles in an organic solvent or water was determined through visual observation. The aqueous nanoparticle systems were studied for stability under various pH values by adjusting the pH of the system using tetramethylammonium hydroxide (TMAOH) and HCl. Zeta-potential analysis (Smoluchowski model) was also performed on all these samples using a Malvern Zetasizer Nano ZS to quantify the stability of the nanoparticle system under different pH conditions.

To determine the surface functionalization of these particles, powder samples of the nanoparticles were obtained through lyophilization of the aqueous dispersions (Labconco FreeZone 4.5), and using nitrogen–drying for the organic nanoparticle dispersions. Fourier Transform Infrared (FTIR) spectroscopy was performed using a Nicolet Avatar 360 to investigate the nature of chemical interaction between SSL and the nanoparticle core. A pure KBr pellet was made using a pellet press, and was used as a background for all the readings. To obtain the FTIR transmission spectra, pellets made by mixing the solid nanoparticles with pure KBr were used in the FTIR apparatus.

X-ray diffractometry (XRD) was used to investigate the crystallinity of the synthesize nanoparticles and to check for the presence of impurities. XRD data were obtained through the use of a Bruker D8 diffractometer operated at 40 kV and 40 mA. The sample was prepared by placing a small portion of the iron oxide nanoparticle powder on a glass slide. The diffraction patterns were collected using a step size of 0.01° and 0.1 s/step count time from $10° \leq 2\theta \leq 80°$. The obtained peaks were compared to available spectra for known compounds using the International Center for Diffraction Data (ICDD) database to determine the species present.

Thermogravimetric analysis (TGA) of the pure ligand (SSL) and the iron oxide nanoparticles was carried out using a TA Instruments (New Castle, DE) Q500 thermal gravimetric analyzer. The entire experiment was run under a constant flow of argon at a flow rate of 10 mL per min. The furnace was first purged with argon for 30 min followed by taring and by then adding a fixed quantity of sample to the platinum pan. The temperature of the system was then raised from room temperature to 110 °C and held at that temperature for 30 min to ensure that all water from the system was removed. The temperature of the system was then increased slowly at a ramp rate of 5 °C/min to 600 °C, and held at this temperature for 30 min.

Emulsion formation and stability experiments

For the emulsion stability studies, dodecane was used as the oil phase while water, with its pH adjusted using TMAOH and HCl, was used as the aqueous phase. The emulsions were generated by mixing the two phase systems using a Tissue Master homogenizer at 8,000 rpm for 15 s. A 1:1 volume ratio (i.e., volume fraction of oil phase 'Φ' was 0.5) of organic phase to aqueous phase was also maintained for all the experiments. To determine the type of Pickering emulsions (O/W or W/O) generated using the water-soluble and oil-soluble nanoparticles, a preliminary emulsion test was initially performed. For this experiment the pH of the aqueous phase was adjusted to 10 using TMAOH and the concentration of the nanoparticle solutions was adjusted to 0.1 wt% using TGA analysis. Nanoparticle solutions of a known volume and weight were first added to a platinum TGA pan which was then loaded into the TGA device. The system was then heated to 600 °C under a steady flow of argon. The residual weight on the pan determined the amount of iron oxide present in solution (since the solvent and ligands would be completely removed at 600 °C). These emulsions were then colored using Acid Blue 9 dye, which preferentially colors the aqueous phase, and optical microscopy images of the emulsions formed using the oil-soluble and water-soluble particles were obtained using a National 163 optical microscope fitted with a custom digital imaging apparatus. The two phase mixtures were mixed using the homogenizer for 15 s after which 100 μL samples were immediately drawn using a micropipette. These samples were added on top of a sterile glass slide and covered with a glass cover slip to obtain optical microscopy images.

Studies for pH and salinity responsiveness of the dodecane-in-water emulsions were also carried out at the same conditions ($\Phi = 0.5$). TMAOH/HCl was used to adjust the pH and pure NaCl was used to adjust the salinity of the samples. The pH of the system was

varied from 6 to 12 and the salinity was varied from 0.1 to 3.5 wt% NaCl. Optical microscopy was carried out on the samples immediately after mixing, as well as 10 days after mixing, to determine the reduction in emulsion stability over time. To understand the influence of surfactant and iron oxide nanoparticles independently on emulsion stability, a simple experiment using the emulsions and a permanent magnet was carried out. The emulsion systems at the different pH values were generated using the SL coated particles and were kept undisturbed for 10 days after mixing using the homogenizer in the same way as performed for the pH-responsiveness study. These emulsion systems were then exposed to a strong permanent magnet and were kept in contact with the magnet for 24 h. This drove the magnetic iron oxide nanoparticles to the bottom of the vial and removed some of the nanoparticles which were influencing emulsion stability. The emulsion stability at this reduced concentration of iron oxide nanoparticles was then noted visually and photographic evidence was obtained for the same.

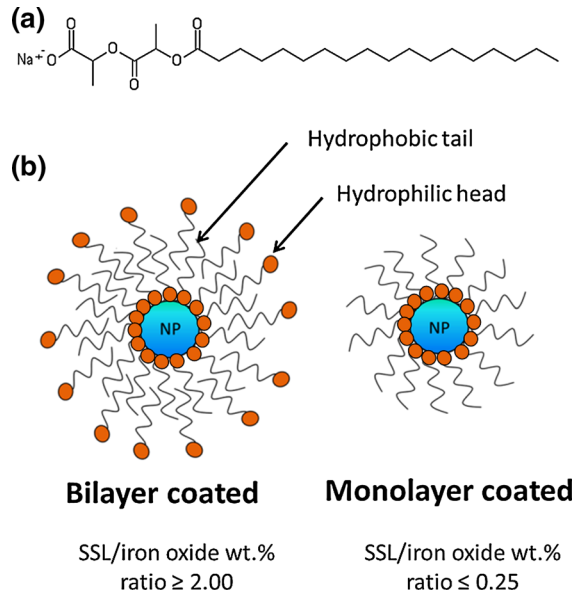

Fig. 1 **a** Chemical structure of sodium stearoyl lactylate (SSL), **b** Generation of monolayer and bilayer coated SSL particles depending upon the amount of SSL added to the reaction system

Results and discussion

Preparation and characterization of SL coated iron oxide nanoparticles

The coprecipitation method is a popular choice for researchers to easily synthesize iron oxide nanoparticles due to the low cost of precursors and relatively low reaction temperatures required. It is easy to achieve gram scale quantities of nanoparticles by using the coprecipitation method even though the synthesized samples are usually polydisperse in nature. Iron oxide nanoparticles synthesized using the coprecipitation method have been surface functionalized with agents like oleic acid, dextrin, etc. for use in various specialized applications.(Babes et al. 1999; Kim et al. 2001; Predoi 2007) Upon synthesis of SL coated iron oxide nanoparticles with varying amounts of SSL, it was observed that at lower SSL concentrations (ligand: iron oxide ratio by weight <0.5) the synthesized particles are readily dispersible in an organic solvent like hexane, while at higher concentrations (ligand: iron oxide ratio by weight >1.0) the particles are dispersible in water. At intermediate concentrations (0.5–1.0), while some of the particles are dispersible in hexane or water, there are also a significant number of particles which are unstable and precipitate from solution. This leads us to conclude that at lower concentrations of SSL there is just enough of the ligand to coat the iron oxide core with a monolayer, leaving the hydrophobic alkyl tails/chains extended into the solvent, making the particles dispersible in organic solvents. At higher concentrations, there is enough SSL in solution for the hydrophobic tails of the free ligand in solution to interact with the hydrophobic tails of the attached ligand to form a bilayer structure, as shown in Fig. 1. This would leave the polar head group of SSL (Fig. 1) to be extended in solution, leading to the solubility of these nanoparticles in water. At the intermediate concentrations, there is enough SSL to create a monolayer but not enough SSL to form bilayers which could cause the particles to aggregate into large unstable structures which precipitate from solution. Only the particles synthesized using 400 mg SSL were used for the emulsion studies in this paper. These particles were selected because it is not desirable to have excess SSL in solution since we want the emulsions to be particle stabilized and not SSL stabilized. The presence of excess SSL in solution could also lead to the formation of micelles within the

solution (CMC of SSL ≈0.1 wt%) (Kurukji et al. 2013; Meshram and Jadhav 2012) which would be undesirable.

Through TEM imaging of the monolayer and bilayer particles it was shown that the iron oxide nanoparticle core size was approximately 10 nm for both the monolayer and bilayer coated particles. TEM images of the monolayer and bilayer particles are shown in Online Resource Fig. S1. The core diameters determined via TEM are listed in the Table 1. Table 1 illustrates that the particles are relatively polydisperse in nature. Dynamic light scattering studies show that

Table 1 Stability, solubility, and particle size results for iron oxide nanoparticles synthesized in the presence of varying amounts of SSL

SSL Amount (mg)	Wt. of ligand/wt. of iron oxide	Solubility (hexane/water)	Stability	Nanoparticle core size (nm) TEM	Hydrodynamic diameter (nm) DLS (*volume weighted*)
25	0.125	Hexane	Stable	8.8 ± 4.2	23.7 ± 9.3
50	0.250	Hexane	Stable	10.8 ± 4.2	27.2 ± 7.4
100	0.500	N/A[a]	Unstable	N/A	N/A
200	1.00	N/A[a]	Unstable	N/A	N/A
400	2.00	Water	Stable	9.9 ± 4.9	39.1 ± 23.5
600	3.00	Water	Stable	7.8 ± 4.4	35.1 ± 24.8
800	4.00	Water	Stable	9.8 ± 5.4	38.0 ± 27.7

[a] At these SSL concentrations some particles were stable in hexane but a majority of the particles formed aggregates and precipitated out of solution

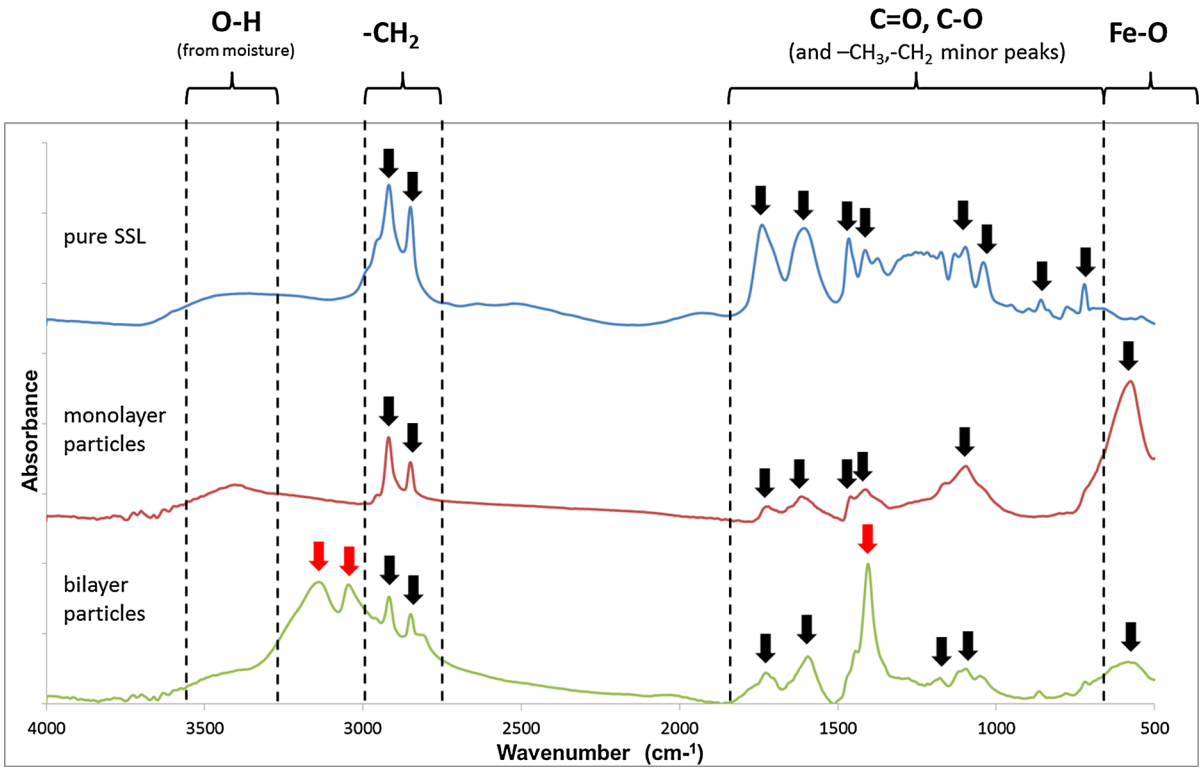

Fig. 2 FTIR spectra for pure SSL, SL monolayer iron oxide particles, and SL bilayer iron oxide particles. *Black arrows* analyzed peaks, *red arrows* impurity peaks. (Color figure online)

the hydrodynamic diameter of the monolayer particles is approximately 25 nm while that of the bilayer particles is around 37 nm. Due to the high polydispersity of the samples being studied, and the difference in the associated hydration shell inherent to a DLS measurement (Prakash et al. 2009), the difference in the hydrodynamic diameters cannot be conclusively attributed to factors such as the larger thickness of the bilayer (due to interpenetration of the SL molecules) (Yang et al. 2010).

The FTIR spectra obtained for the pure SSL, the SL monolayer coated particles and the SL bilayer particles are shown in Fig. 2. A detailed analysis of the FTIR spectra is also shown in Table 2. The FTIR spectrum of pure SSL shows characteristic CH_2 bands (from the alkyl group in SSL) (Nakamoto 1997a) at 2,918 and 2,850 cm^{-1}. Similar bands are also seen in the spectra for the SL monolayer and bilayer coated iron oxide nanoparticles. The spectra for pure SSL and the SL monolayer particles also have a CH_3 umbrella mode peak (Wu et al. 2004) at 1,411 cm^{-1}. The FTIR spectrum of the SL monolayer coated particles was compared to the FTIR spectrum of pure SSL so as to analyze how the SSL attaches to the iron oxide core. By analyzing the C = O ester peak (Larkin 2011) (1,739 cm^{-1}) present in the pure SSL spectrum and comparing it to the conjugated C=O peak in the SL monolayer coated particle spectrum it is possible to determine how the C=O groups conjugate with the iron oxide surface. (Nakamoto 1997b) The splitting of the 1,739 cm^{-1} C=O stretch in pure SSL into two peaks at 1,718 cm^{-1} and 1,614 cm^{-1} (Δ or difference in the wavelengths after splitting = 104 cm^{-1}) in the SL monolayer spectrum hints at a bidentate type of bridging being present in the system (Liu et al. 2008; Nakamoto 1997b). Such type of attachment of surfactants to nanoparticles has been shown before in other studies (Shukla et al. 2003).

However, due to the sheer number of C=O and C–O interactions present in the SSL molecule it is not possible to definitively determine which of the carbonyl carbons interacts with the iron oxide surface. It is interesting to note that the FTIR spectrum for the SL bilayer coated nanoparticles shows the presence of NH_4^+ impurities present in the bilayer coated nanoparticle system (Fig. 2, red arrows). The ammonium ion peaks (3,140, 3,046 and 1,404 cm^{-1}) (Larkin 2011) are possibly a result of NH_4Cl being generated in the system during synthesis. Usually during the coprecipitation method, the ammonium hydroxide will be converted to ammonia due to the relatively high temperature and high pH of the system. The ammonia vapors are then removed by the nitrogen flowing over the system. However, commercial grade SSL contains free lactic acid which can cause localized reductions in pH in the reaction vessel. This will shift the ammonia formation reaction equilibrium toward the reactants, thereby releasing ammonium ions in solution. (Yeh et al. 2005) These ammonium ions can then combine with the free chloride ions from the iron salts and generate water-soluble ammonium chloride. XRD analysis of the lyophilized water-soluble particles (Fig. 3) shows that the particles are primarily Fe_3O_4 and also confirms the presence of these ammonium chloride impurities. The purification

Table 2 Details for FTIR peaks of pure SSL, SL monolayer iron oxide particles and SL bilayer iron oxide particles

Species	Peak position (cm^{-1})	Interaction[a]
Pure SSL	2,918	(–CH_2 stretch) *symmetric*
	2,850	(–CH_2 stretch) *asymmetric*
	1,739	(C=O stretch) from R-CO–O-R
	1,605	(C=O stretch) from R-CO_2^-
	1,465	(–CH_2 bend)
	1,411	(–CH_3 umbrella mode)
	1,095	(C–O stretch) from R–CO–O–R
	1,037	(C–O stretch) from R–CO–O–R
	721	(–CH_2 rocking)
SL monolayer nanoparticles	2,919	(–CH_2 stretch) *symmetric*
	2,850	(–CH_2 stretch) *asymmetric*
	1,718	(C=O stretch) *conjugated*
	1,614	(C–O stretch) *conjugated*
	1,461	(–CH_2 bend)
	1,411	(–CH_3 umbrella mode)
	1,096	(C–O stretch) from R–CO–O–R
	575	(Fe–O stretch)
SL bilayer nanoparticles	3,140	(NH_4 stretch) *asymmetric*
	3,046	(NH_4 stretch) *symmetric*
	2,917	(–CH_2 stretch) *symmetric*
	2,849	(–CH_2 stretch) *asymmetric*
	1,727	(C=O stretch) *conjugated*
	1,594	(C–O stretch) from R-CO_2^-
	1,404	(NH_4 bend)
	1,177	(C–O stretch) from R-CO–O-R
	1,095	(C–O stretch) from R-CO–O-R
	582	(Fe–O stretch)

[a] Sources used for analysis: (Larkin 2011; Nakamoto 1997a, b; Smith 1998; Wu et al. 2004)

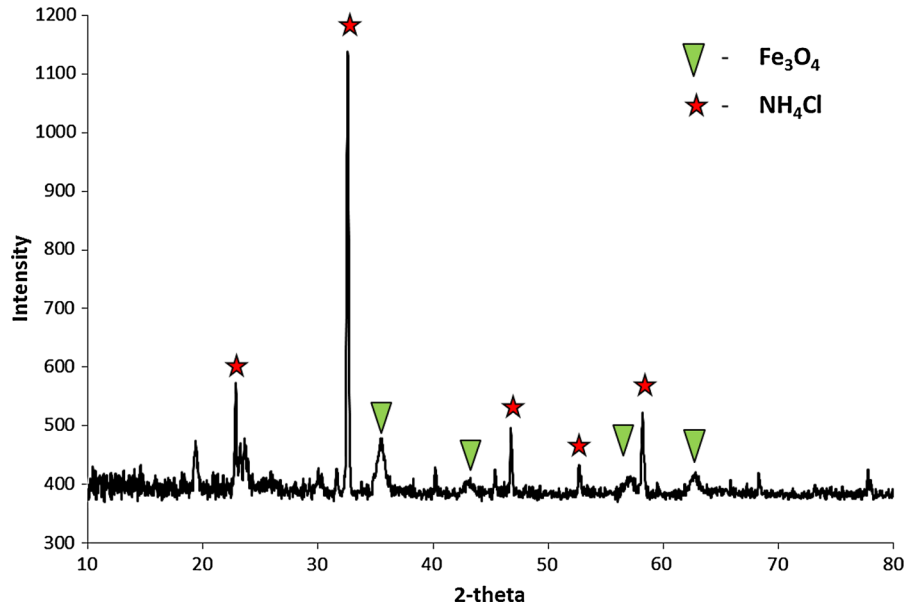

Fig. 3 XRD spectrum for SL bilayer coated iron oxide nanoparticles

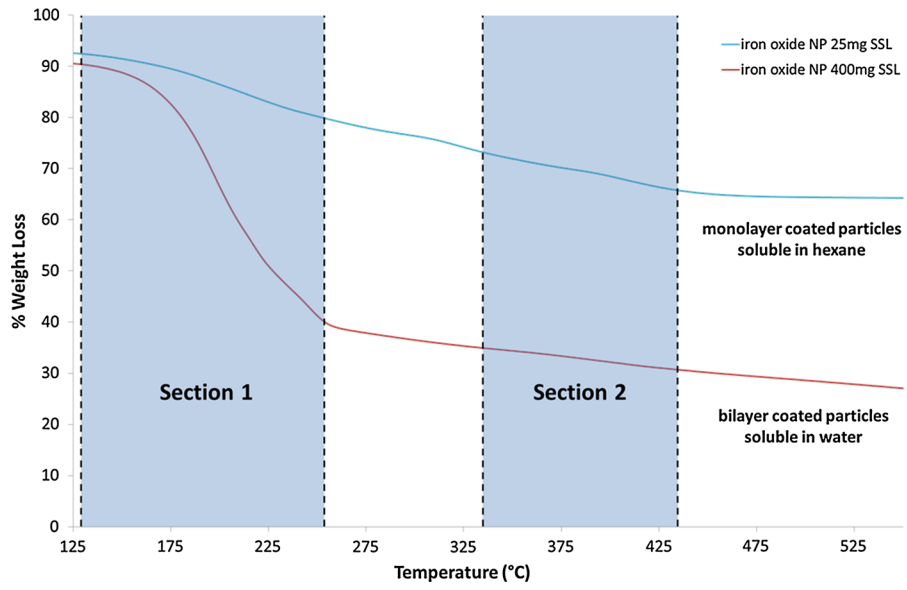

Fig. 4 TGA curves of SL monolayer/bilayer coated iron oxide nanoparticles

processes of dialysis and centrifugal ultrafiltration are successful in removing most of the ammonium chloride, but a small amount of ammonium chloride impurities do remain in the system and are visible in the FTIR and XRD results due to the high sensitivity of these techniques.

Even though the solubility results and FTIR results suggest the presence of a bilayer on the particles synthesized with higher amounts of SSL, thermogravimetric analysis (TGA) was also performed on the particles to confirm the presence of a bilayer. The TGA curves shown in Fig. 4 shows that the release of molecules upon increase in temperature is split into two bands or sections, namely Section 1: where any free lactic acid (boiling point: 122 °C) and SSL (flash point: 221 °C) are removed from the particles and Section 2: where the layer of surfactant molecules attached to the iron oxide core is released. It is also important to note that the position of Section 2 is around 376 °C which is the boiling point of stearic

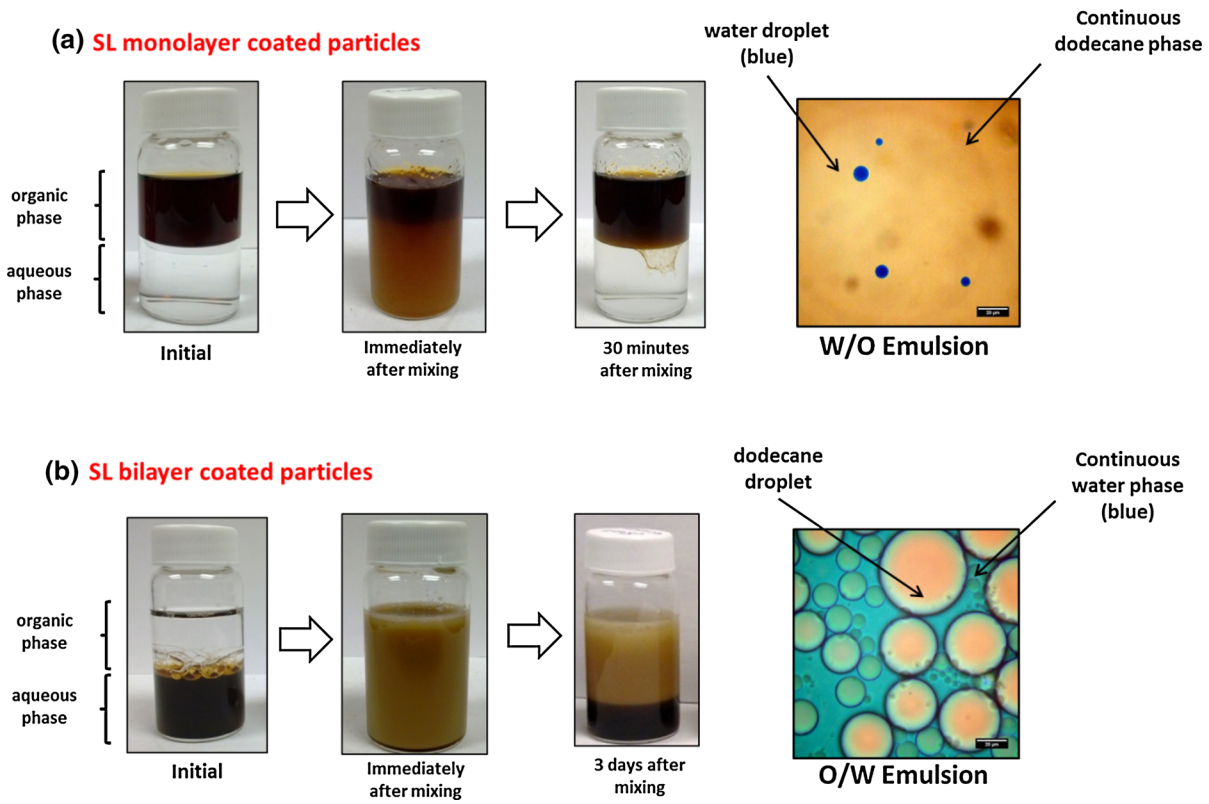

Fig. 5 Preliminary Pickering emulsion experiments using **a** SL monolayer and **b** SL bilayer coated iron oxide nanoparticles. (pH of aqueous phase = 10 and iron oxide nanoparticle concentration = 0.1 wt%)

acid and most of the weight loss in this section can be attributed to the removal of attached surfactant (which should be similar to stearic acid due to the conjugated C=O groups) from the iron oxide core. Also, since the decomposition sublimation of ammonium chloride starts at around 338 °C and an increased reduction in weight is not observed after that point, one can safely say that a significant quantity of ammonium chloride is not present in the system.

From the TGA results in Fig. 4, it is evident that the water-soluble particles synthesized at higher concentrations of SSL (400 mg) have a much higher % weight loss in Section 1 (≈50 %) compared to the hexane-soluble particles synthesized at lower concentrations of SSL (25 mg) (≈10 %). The TGA results for the other concentrations of SSL follow the trends listed above and are shown in Online Resource Fig. S2. Hence, we can deduce that the particles synthesized at higher concentrations of SSL have relatively more SSL molecules loosely associated to the nanoparticle (i.e., held via ligand–ligand/ligand–solvent interactions) compared to the particles synthesized at lower concentrations of SSL, which have a higher fraction of ligand molecules attached to the iron oxide core. This adds more evidence to our analysis that at higher SSL concentrations, bilayers are present in the system. It should be noted that even though most of the SSL should be associated with the nanoparticle in the aqueous dispersions, the presence of a small amount of SSL micelles in solution is inevitable. The presence of these SSL micelles in solution could slightly improve the emulsion forming capacity of the iron oxide system under investigation since a very small fraction of the overall emulsion could be stabilized by these micelles themselves.

Application of SL coated iron oxide nanoparticles in Pickering emulsions

The results from the preliminary emulsion formation experiments carried out (at pH value 10) using the SL monolayer and bilayer coated particles are shown in Fig. 5. For the SL monolayer coated nanoparticles (dispersible in organic phase) it was observed

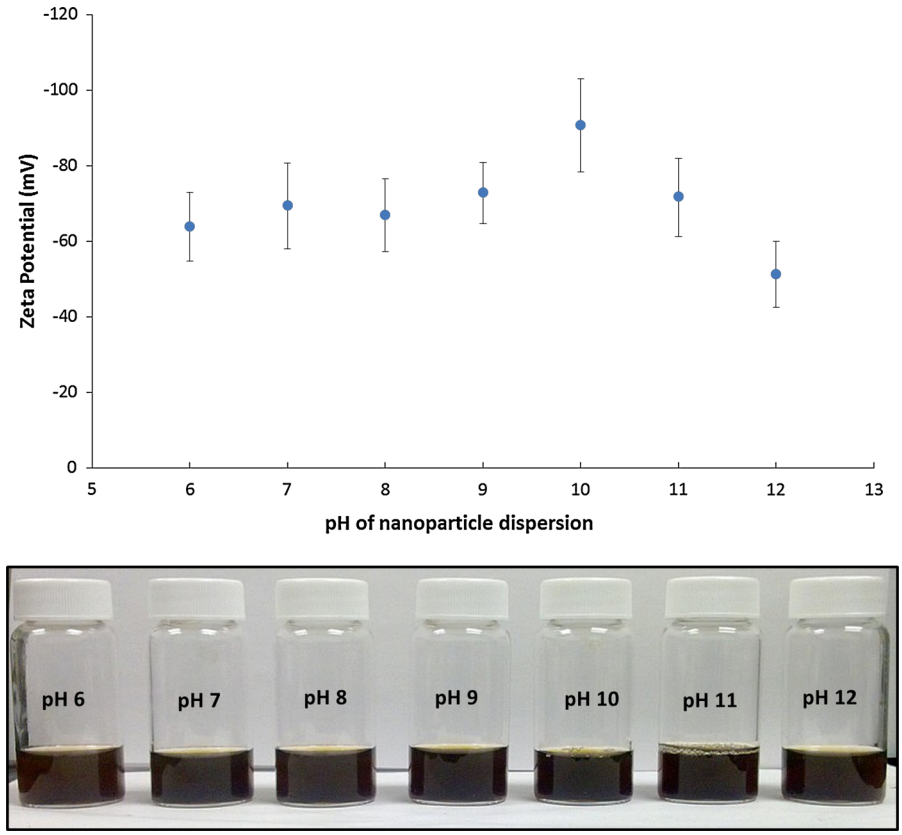

Fig. 6 Stability analysis using zeta-potential of SL bilayer coated iron oxide nanoparticles at various pH values

(Fig. 5a) post-mixing that an extremely unstable emulsion was generated. This emulsion separated into two phases over a period of 30 min. Before complete phase separation was achieved, we were able to obtain optical microscopy images using Acid Blue 9 water soluble dye to determine the type of emulsion formed. From the presence of water droplets (blue) dispersed in the organic phase (brown) in the optical microscopy image (Fig. 5a) one can see that these monolayer coated particles generate extremely unstable water-in-oil (W/O) emulsions. Note that since the emulsion is extremely unstable with droplets coalescing frequently, it is difficult to get clear optical microscopy images. In contrast, a relatively stable emulsion was obtained post-mixing, for the SL bilayer coated nanoparticles (dispersible in aqueous phase), as is seen in Fig. 5b. Upon optical microscopy analysis of this emulsion in the presence of Acid Blue 9 dye, the presence of dodecane droplets (brown) dispersed in water (blue) is clearly visible in Fig. 5b. This indicates the successful formation of oil-in-water (O/W) Pickering emulsions through the use of SL bilayer coated iron oxide nanoparticles. These findings match those expected from following the Bancroft rule (i.e., the phase in which the stabilizing agent is more soluble will be the continuous phase) (Davies 1957) and directs us toward using the SL bilayer coated nanoparticles in our next set of Pickering emulsion studies.

Zeta-potential analysis of the 400 mg SL coated iron oxide nanoparticles dispersed in water at different pH values (adjusted using TMAOH) is presented in Fig. 6, where the error bars represent the standard error of the mean from triplicate measurements at each pH value.

A modest increase in zeta-potential was observed from pH 6 to pH 10 (Fig. 6). The fact that the particles are stable at a pH of 7, which is approximately the isoelectric point for uncoated iron oxide nanoparticles, is further proof for the presence of a charged bilayer being present on the particle core (Ingram et al. 2010). Upon further increase in pH (pH >10) however, a drop in zeta-potential was observed. This trend in zeta-potential is similar to that observed by Lan et al. (Lan et al. 2007) for oleic acid bilayer coated iron oxide

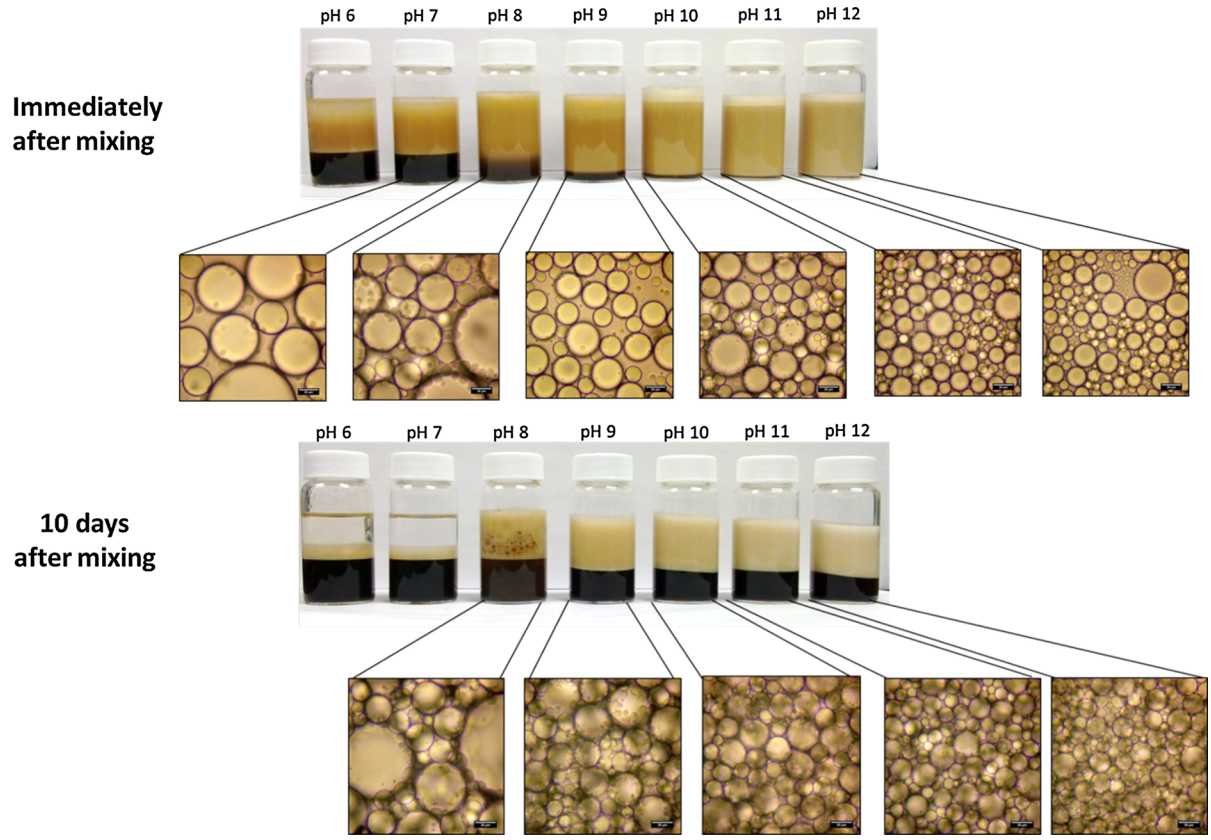

Fig. 7 pH-responsiveness studies on oil-in-water Pickering emulsions generated using SL bilayer coated iron oxide nanoparticles

nanoparticles where a drop in zeta-potential was observed for a pH value of 12.5, and this behavior was attributed to the desorption of the secondary oleic acid layer. Hence, due to the similarity between the stabilizing agent conjugation and structure (oleic acid and SSL), the reduction in zeta-potential (at a pH >10), can also be attributed to the possible desorption of the outer SSL layer in this case of SL bilayer coated nanoparticles. This desorption occurs due to the strong hydration of the hydrophilic head groups and weakening van der Waals forces (between the interacting hydrophobic tail groups) in an alkaline environment. (Fu et al. 2001; Lan et al. 2007; Shen et al. 1999; Zhou et al. 2012).

The results obtained from the pH-responsiveness experiment on Pickering emulsions stabilized using the SL bilayer coated particles are shown in Fig. 7. As mentioned before, the iron oxide concentration in the aqueous phase was maintained at 0.1 wt. % using TGA analysis for the samples in this experiment. Immediately upon mixing, emulsions were formed with the SL bilayer particles at all of the seven pH values studied. Optical microscopy of these emulsions shows that at the higher pH values (pH $\geq$9) the oil droplet size in the O/W emulsions is approximately 20 μm while at lower pH values (pH $\leq$8) the droplet size is slightly larger at around 35 μm. The visibly larger droplets (formed due to due to rapid coalescence after mixing) for the samples at the lower pH values are proof that the emulsions at the lower pH values are not being stabilized to a large extent (compared to the samples at high pH values). By observing the samples and their optical microscopy images after an extended period of time (10 days), a clear trend in stability is observed over the range of pH values studied. At the acidic and neutral pH values the carboxylate groups are protonated resulting in a reduction in interfacial activity for the particles. (Ingram et al. 2010) The emulsions at pH 6 and pH 7 almost completely separate into the original oil and water phases, while

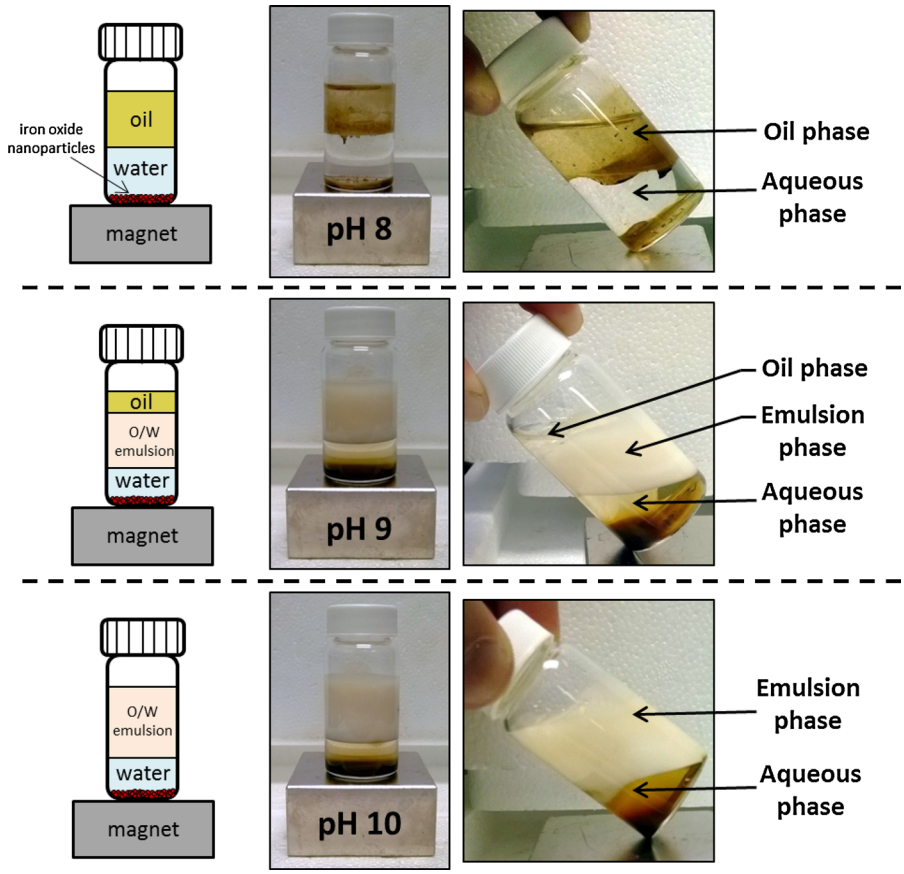

Fig. 8 Effect of a permanent magnet on emulsion stability at various pH values

the emulsion at pH 8 has an abundance of larger sized droplets. Creaming is also observed at the pH values where stable emulsions are obtained (pH $\geq$8). This is also confirmed by the increased density of droplets visualized in the optical microscopy images. The stable emulsion volume fraction is around 50 % which is common for similar systems with O/W ratios of 1:1. (Lan et al. 2007) The color of iron oxide nanoparticles in the emulsions also confirmed their role in emulsion stability. This trend in stability is very similar to that obtained by other studies (Ingram et al. 2010; Lan et al. 2007) on oleic acid bilayer coated iron oxide nanoparticles. From the zeta-potential analysis results and the pH-responsiveness study, one can hypothesize that while the particles stabilize the emulsions at neutral and borderline basic pH, at higher pH values the emulsions are possibly stabilized by both the particles and the free surfactant (SSL). At acidic and neutral pH (pH 6 and 7), the protonation of the carboxylic groups combined with the lack of free SSL could result in the destabilization observed in Fig. 8. At pH values of 8, 9, and 10, the O/W emulsions could be stabilized by the bilayer coated nanoparticles, but at the higher pH values of 11 and 12, it is possible that the desorbed surfactant can be stabilizing the emulsions along with the nanoparticles.

This type of synergistic stabilization of O/W emulsions by nanoparticles and surfactants has been seen previously in other nanoparticle-surfactant systems (Eskandar et al. 2007; Zou et al. 2013) and has been hypothesized to occur due to competitive adsorption of particles and desorbed surfactant molecules in bilayer systems (Lan et al. 2007).

The simple test using a permanent magnet (Fig. 8) shows us that the emulsions at the pH values studied respond differently under the influence of a magnetic field. For the sample at pH 8, the emulsion is destabilized (due to removal of the magnetic iron

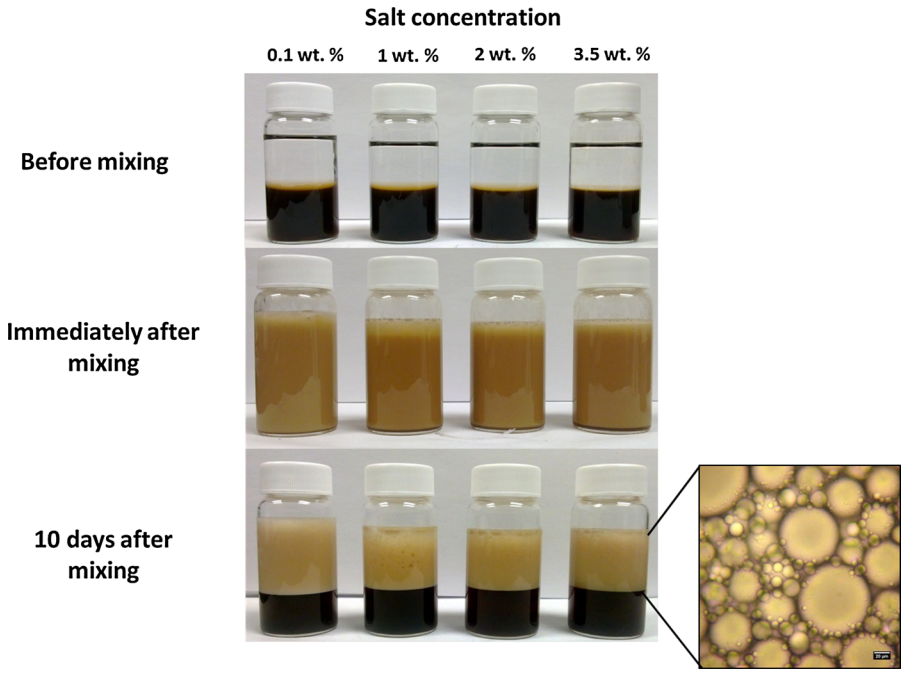

Fig. 9 Salinity studies on oil-in-water Pickering emulsions generated using SL bilayer coated iron oxide nanoparticles. (pH of aqueous phase before salt addition = 7.5 and iron oxide nanoparticle concentration = 0.1 wt%)

oxide nanoparticles) and the oil droplets coalesce to give a distinct oil phase and water phase. For the emulsion sample at pH of 9, a few oil droplets in the emulsion phase coalesce and form a distinct layer of dodecane at the top of the emulsion phase. However, there is still an emulsion phase present in the system. The emulsion sample at pH 10 remains relatively stable under the influence of the magnetic field and no visual evidence of dodecane droplet coalescence in the emulsion phase is observed. At higher pH values, the magnet has an effect on emulsion stability similar to that observed at pH 10 (i.e., no visual evidence of a distinct oil phase). This lends credence to our previous hypothesis that at higher pH values the emulsion may be co-stabilized by the nanoparticles and the surfactant (SSL). It is important to note that the smaller iron oxide nanoparticles will not be influenced by the magnetic field and will still remain dispersed in the emulsion/organic phase (as is visible from the brownish iron oxide color of the emulsion in Fig. 8). While it is difficult to reach a definitive conclusion without the aid of detailed interfacial studies on these systems, the magnetic effect on emulsion stability does indicate surfactant/nanoparticle co-stabilization at higher pH values.

Salinity studies carried out using salt concentrations from 0.1 to 3.5 wt% are shown in Fig. 9. From visual observation it is clear that the emulsions are stable at all of the salt concentrations studied. Over a period of 10 days, creaming is observed in all the samples and the stable emulsion volume fraction is around 50 %, similar to that witnessed in the previous pH-responsiveness studies. A small degree of coalescence is, however, observed for the samples with the salt concentration above 0.1 wt%. Optical microscopy on these samples revealed a significant quantity of larger sized droplets (droplet size >50 μm). At higher salt concentrations, the presence of Na^+ ions in solution has a similar effect to the presence of H^+ ions in an acidic solution and causes the carboxylate groups to associate with the ions, hence decreasing double layer thickness. This combined with competitive adsorption of particles and desorbed surfactant molecules results in a change in the wettability of the particles. (Binks et al. 2006; Ingram et al. 2010; Lan et al. 2007) This results in the larger droplet size being present, thereby aiding emulsion destabilization. There is a possibility that the destabilizing effect of the salt is being countered by the fact that stearoyl lactylate (SL) in presence of a sodium counter ion (i.e.,

SSL) has been shown to have a better interfacial tension reduction capacity. This phenomenon has been attributed in literature to the difference in micellar aggregation behavior of SL and SSL.(Meshram and Jadhav 2012) This proposed micellar aggregation behavior could explain relatively high stability (compared to oleic acid bilayer particles) (Ingram et al. 2010) of the Pickering emulsions generated using SL bilayer coated nanoparticles in the presence of significant salt concentrations.

Conclusion

Iron oxide nanoparticles were synthesized using a co-precipitation technique and their surfaces were successfully functionalized with monolayers and bilayers of the stearoyl lactylate (SL). The presence of a monolayer or bilayer was dependent upon the amount of the surfactant SSL introduced into the system during synthesis. Characterization using various analytical techniques confirmed that the particles were primarily Fe_3O_4 iron oxide nanoparticles with the SL molecules attached to the nanoparticle core via a bidentate type chelating complex. Small quantities of ammonium chloride impurities are present in the synthesized particles which are reduced in concentration via various purification methods. Preliminary studies showed that the SL monolayer coated particles generated unstable W/O emulsions, while the SL bilayer coated particles generated relatively stable O/W emulsions. Dispersions of the synthesized SL bilayer coated nanoparticles in water were stable over an extended period of time at pH values varying from 6 to 12. O/W Pickering emulsions were also successfully generated using the SL bilayer coated iron oxide nanoparticles at extremely low iron oxide concentrations (0.1 wt%). The pH-responsiveness studies on emulsions systems stabilized by these particles showed that these particles were successful at stabilizing O/W emulsions at pH values from 8 and 12. At acidic and neutral pH values the emulsions coalesced into distinct oil and water phases due to protonation of bilayers on the particles. These trends in pH-responsiveness are comparable to those reported previously by other researchers in similar bilayer systems.(Ingram et al. 2010; Lan et al. 2007) The trends in emulsion stability combined with zeta-potential analysis on the nanoparticle dispersions and the simple magnetic test hint to a co-stabilization of the emulsions by the nanoparticle and the desorbed surfactant at various pH values. Salinity studies also showed that emulsions stabilized using the bilayer coated particles were stable over an extended period of time at salt concentrations ranging from 0.1 to 3.5 wt%.

Thus, from this study, we have demonstrated the capacity to functionalize iron oxide nanoparticles with a benign surfactant and tested its effectiveness in stabilizing O/W Pickering emulsions at various pH and salinity conditions. This study provides fundamental insights into the capacity to multi-functionalize nanoparticles and Pickering emulsions generated using such particles could be used in the future for applications like oil-spill cleanup.

Acknowledgements This research was made possible in part from a grant from The Gulf of Mexico Research Initiative through the Consortium for Molecular Engineering of Dispersant Systems (CMEDS). The authors also thank Dr. Michael Miller and the Auburn University Research and Instrumentation Facility for access to the transmission electron microscope. The authors also greatly appreciate the assistance in the use of characterization equipment by Dr. Allan David, Dr. Virginia Davis, and Steven Moore at Auburn University.

References

Andreas K, Georgieva R, Ladwig M et al (2012) Highly efficient magnetic stem cell labeling with citrate-coated superparamagnetic iron oxide nanoparticles for MRI tracking. Biomaterials 33:25–4515. doi:10.1016/j.biomaterials.2012.02.064

Avdeev MV, Mucha B, Lamszus K et al (2010) Structure and in vitro biological testing of water-based ferrofluids stabilized by monocarboxylic acids. Langmuir 26:9–8503. doi:10.1021/la904471f

Babes L, Denizot B, Tanguy G et al (1999) Synthesis of iron oxide nanoparticles used as MRI contrast agents: a parametric study. J Colloid Interface Sci 212:474–482. doi:10.1006/jcis.1998.6053

Binks BP, Lumsdon SO (2001) Pickering emulsions stabilized by monodisperse latex particles: effects of particle size. Langmuir 17:4540–4547. doi:10.1021/la0103822

Binks BP, Whitby CP (2005) Nanoparticle silica-stabilised oil-in-water emulsions: improving emulsion stability. Colloids Surf A 253:105–115. doi:10.1016/j.colsurfa.2004.10.116

Binks BP, Murakami R, Armes SP, Fujii S (2006) Effects of pH and salt concentration on oil-in-water emulsions stabilized solely by nanocomposite microgel particles. Langmuir 22:7–2050. doi:10.1021/la053017+

Brown P, Bushmelev A, Butts CP et al (2012) Magnetic control over liquid surface properties with responsive surfactants. Angew Chem Int Ed Engl 51:6–2414. doi:10.1002/anie.201108010

Chen T, Colver PJ, Bon SAF (2007) Organic–inorganic hybrid hollow spheres prepared from TiO_2-stabilized Pickering emulsion polymerization. Adv Mater 19:2286–2289. doi:10.1002/adma.200602447

Chen W, Liu X, Liu Y, Kim H-I (2010) Synthesis of microcapsules with polystyrene/ZnO hybrid shell by Pickering emulsion polymerization. Colloid Polym Sci 288:1393–1399. doi:10.1007/s00396-010-2277-8

Davies J (1957) A quantitative kinetic theory of emulsion type, I. Physical chemistry of the emulsifying agent. In: Proceedings of the Second International Congress of Surface Activity London, pp 426–438

Eskandar N, Simovic S, Prestidge C (2007) Synergistic effect of silica nanoparticles and charged surfactants in the formation and stability of submicron oil-in-water emulsions. Phys Chem Chem 9:6313–6318. doi:10.1039/b705094a

European Food Safety Authority (2013) EFSA ANS panel (EFSA panel on food additives and nutrient sources added to food), 2013: scientific opinion on the re-evaluation of sodium stearoyl-2-lactylate (E 481) and calcium stearoyl-2-lactylate (E 482) as food additives. EFSA J 11:1–35. doi:10.2903/j.efsa.2013.3144

Flores M, Giner E, Fiszman SM et al (2007) Effect of a new emulsifier containing sodium stearoyl-2-lactylate and carrageenan on the functionality of meat emulsion systems. Meat Sci 76:9–18. doi:10.1016/j.meatsci.2006.06.032

Fu L, Dravid VP, Johnson DL (2001) Self-assembled (SA) bilayer molecular coating on magnetic nanoparticles. Appl Surf Sci 181:173–178. doi:10.1016/S0169-4332(01)00388-9

Grigoriev DO, Leser ME, Michel M, Miller R (2007) Mixed micelles as delivery systems for enhanced emulsifier adsorption at the air/water interface: sodium stearoyl lactylate (SSL)/Tween80 solutions. Colloids Surf A 301:158–165. doi:10.1016/j.colsurfa.2006.12.048

He Y, Yu X (2007) Preparation of silica nanoparticle-armored polyaniline microspheres in a Pickering emulsion. Mater Lett 61:2071–2074. doi:10.1016/j.matlet.2006.08.018

Hong RY, Feng B, Chen LL et al (2008) Synthesis, characterization and MRI application of dextran-coated Fe3O4 magnetic nanoparticles. Biochem Eng J 42:290–300. doi:10.1016/j.bej.2008.07.009

Hosseinian A, Rezaei H, Mahjoub A (2011) Preparation of nanosized iron oxide and their photocatalytic properties for congo red. World Acedemy Sci Eng Technol 52:736–739

Hu F, Jia Q, Li Y, Gao M (2011) Facile synthesis of ultrasmall PEGylated iron oxide nanoparticles for dual-contrast T(1)- and T(2)-weighted magnetic resonance imaging. Nanotechnology 22:245604. doi:10.1088/0957-4484/22/24/245604

Ingram DR, Kotsmar C, Yoon KY et al (2010) Superparamagnetic nanoclusters coated with oleic acid bilayers for stabilization of emulsions of water and oil at low concentration. J Colloid Interface Sci 351:32–225. doi:10.1016/j.jcis.2010.06.048

Jain TK, Morales MA, Sahoo SK et al (2005) Iron oxide nanoparticles for sustained delivery of anticancer agents. Mol Pharm 2:194–205. doi:10.1021/mp0500014

Katepalli H, John VT, Bose A (2013) The response of carbon black stabilized oil-in-water emulsions to the addition of surfactant solutions. Langmuir 29:7–6790. doi:10.1021/la400037c

Khedr MH, Abdel Halim KS, Soliman NK (2009) Synthesis and photocatalytic activity of nano-sized iron oxides. Mater Lett 63:598–601. doi:10.1016/j.matlet.2008.11.050

Kim DK, Zhang Y, Voit W et al (2001) Synthesis and characterization of surfactant-coated superparamagnetic monodispersed iron oxide nanoparticles. J Magn Magn Mater 225:30–36. doi:10.1016/S0304-8853(00)01224-5

Kokelaar J, Garritsen J, Prins A (1995) Surface rheological properties of sodium stearoyl-2-lactylate (SSL) and diacetyl tartaric esters of mono (and di) glyceride (DATEM) surfactants after a mechanical surface treatment in relation to their bread improving abilities. Colloids Surf A 95:69–77

Kurukji D, Pichot R, Spyropoulos F, Norton IT (2013) Interfacial behaviour of sodium stearoyllactylate (SSL) as an oil-in-water Pickering emulsion stabiliser. J Colloid Interface Sci 409:88–97. doi:10.1016/j.jcis.2013.07.016

Kwak B (2005) Synthesis of MRI contrast agent by coating superparamagnetic iron oxide with chitosan. IEEE Trans Magn 41:4102–4104. doi:10.1109/TMAG.2005.855338

Lamb J, Hentz K, Schmitt D et al (2010) A one-year oral toxicity study of sodium stearoyl lactylate (SSL) in rats. Food Chem Toxicol 48:9–2663. doi:10.1016/j.fct.2010.06.037

Lan Q, Liu C, Yang F et al (2007) Synthesis of bilayer oleic acid-coated Fe_3O_4 nanoparticles and their application in pH-responsive Pickering emulsions. J Colloid Interface Sci 310:9–260. doi:10.1016/j.jcis.2007.01.081

Larkin P (2011) Infrared and Raman spectroscopy; principles and spectral interpretation. Elsevier, New York

Li J, Stöver HDH (2008) Doubly pH-responsive Pickering emulsion. Langmuir 24:40–13237. doi:10.1021/la802619m

Liu J, He F, Durham E et al (2008) Polysugar-stabilized Pd nanoparticles exhibiting high catalytic activities for hydrodechlorination of environmentally deleterious trichloroethylene. Langmuir 24:36–328. doi:10.1021/la702731h

Lodhia J, Mandarano G, Ferris N et al (2010) Development and use of iron oxide nanoparticles (part 1): synthesis of iron oxide nanoparticles for MRI. Biomed Imaging Interv J. doi:10.2349/biij.6.2.e12

Melle S, Lask M, Fuller GG (2005) Pickering emulsions with controllable stability. Langmuir 21:62–2158. doi:10.1021/la047691n

Meshram P, Jadhav S (2012) Preparation and properties of lactic acid-based modified carboxylic surfactant. J Surf Sci Technol 28:149–161

Morales MA, Jain TK, Labhasetwar V, Leslie-Pelecky DL (2005) Magnetic studies of iron oxide nanoparticles coated with oleic acid and Pluronic® block copolymer. J Appl Phys 97:10Q905. doi:10.1063/1.1850855

Morales M, Finotelli P, Coaquira J et al (2008) In situ synthesis and magnetic studies of iron oxide nanoparticles in calcium–alginate matrix for biomedical applications. Mater Sci Eng, C 28:253–257. doi:10.1016/j.msec.2006.12.016

Nakamoto K (1997a) Infrared and Raman spectra of inorganic and coordination compounds: Part a: theory and applications in inorganic chemistry, 5th edn. Wiley, New York

Nakamoto K (1997b) Infrared and Raman spectra of inorganic and coordination compounds: part b: applications in coordination, organometallic, and bioinorganic chemistry. John Wiley & Sons, Fifth Edit

Orbell JD, Godhino L, Bigger SW et al (1997) Oil spill remediation using magnetic particles: an experiment in

environmental technology. J Chem Educ 74:1446. doi:10.1021/ed074p1446

Orbell JD, Dao HV, Ngeh LN, Bigger SW (2007) Magnetic particle technology in environmental remediation and wildlife rehabilitation. Environmentalist 27:175–182. doi:10.1007/s10669-007-9026-7

Park J-Y, Lee Y-J, Khanna PK et al (2010) Alumina-supported iron oxide nanoparticles as Fischer–Tropsch catalysts: effect of particle size of iron oxide. J Mol Catal A 323:84–90. doi:10.1016/j.molcata.2010.03.025

Prakash A, Zhu H, Jones CJ et al (2009) Bilayers as phase transfer agents for nanocrystals prepared in nonpolar solvents. ACS Nano 3:49–2139. doi:10.1021/nn900373b

Predoi D (2007) A study on iron oxide nanoparticles coated with dextrin obtained by coprecipitation. Dig J Nanomater Biostruct 2:169–173

Qiao R, Yang C, Gao M (2009) Superparamagnetic iron oxide nanoparticles: from preparations to in vivo MRI applications. J Mater Chem 19:6274. doi:10.1039/b902394a

Qiao X, Zhou J, Binks BP et al (2012) Magnetorheological behavior of Pickering emulsions stabilized by surface-modified Fe_3O_4 nanoparticles. Colloids Surf A 412:20–28. doi:10.1016/j.colsurfa.2012.06.026

Saha A, Nikova A, Venkataraman P et al (2013) Oil emulsification using surface-tunable carbon black particles. ACS Appl Mater Interfaces 5:3094–3100

Shen L, Laibinis PEP, Hatton TAT (1999) Bilayer surfactant stabilized magnetic fluids: synthesis and interactions at interfaces. Langmuir 15:447–453. doi:10.1021/la9807661

Shukla N, Liu C, Jones PM, Weller D (2003) FTIR study of surfactant bonding to FePt nanoparticles. J Magn Magn Mater 266:178–184. doi:10.1016/S0304-8853(03)00469-4

Smith B (1998) Infrared spectral interpretation: a systematic approach. CRC Press, Boca Raton

Sovilj V, Milanovic J, Petrovic L (2013) Influence of gelatin–sodium stearoyl lactylate interaction on the rheological properties of gelatin gels. Colloids Surf A 417:211–216. doi:10.1016/j.colsurfa.2012.11.009

Sullivan AP, Kilpatrick PK (2002) The effects of inorganic solid particles on water and crude oil emulsion stability. Ind Eng Chem Res 41:3389–3404. doi:10.1021/ie010927n

Torres Galvis HM, Bitter JH, Khare CB et al (2012) Supported iron nanoparticles as catalysts for sustainable production of lower olefins. Science 335:8–835. doi:10.1126/science.1215614

Wang CY, Hong JM, Chen G et al (2010) Facile method to synthesize oleic acid-capped magnetite nanoparticles. Chin Chem Lett 21:179–182. doi:10.1016/j.cclet.2009.10.024

Whitehurst R (2008) Emulsifiers in food technology. Wiley, New York

Wu N, Fu L, Su M et al (2004) Interaction of fatty acid monolayers with cobalt nanoparticles. Nano Lett 4:383–386. doi:10.1021/nl035139x

Yang K, Peng H, Wen Y, Li N (2010) Re-examination of characteristic FTIR spectrum of secondary layer in bilayer oleic acid-coated Fe_3O_4 nanoparticles. Appl Surf Sci 256:3093–3097. doi:10.1016/j.apsusc.2009.11.079

Yeh JT, Pennline HW, Resnik KP, Rygle K (2005) Semi-batch absorption and regeneration studies for CO_2 capture by aqueous ammonia. Fuel Process Technol 86:1533–1546. doi:10.1016/j.fuproc.2005.01.015

Zhang L, He R, Gu H (2006) Oleic acid coating on the monodisperse magnetite nanoparticles. Appl Surf Sci 253:2611–2617. doi:10.1016/j.apsusc.2006.05.023

Zhang K, Wu W, Guo K et al (2009) Magnetic polymer enhanced hybrid capsules prepared from a novel Pickering emulsion polymerization and their application in controlled drug release. Colloids Surf A 349:110–116. doi:10.1016/j.colsurfa.2009.08.005

Zhou J, Wang L, Qiao X et al (2012) Pickering emulsions stabilized by surface-modified Fe_3O_4 nanoparticles. J Colloid Interface Sci 367:24–213. doi:10.1016/j.jcis.2011.11.001

Zinoviadou KG, Moschakis T, Kiosseoglou V, Biliaderis CG (2011) Impact of emulsifier-polysaccharide interactions on the stability and rheology of stabilised oil-in-water emulsions. Procedia Food Sci 1:57–61. doi:10.1016/j.profoo.2011.09.010

Zou S, Yang Y, Liu H, Wang C (2013) Synergistic stabilization and tunable structures of Pickering high internal phase emulsions by nanoparticles and surfactants. Colloids Surf A 436:1–9. doi:10.1016/j.colsurfa.2013.06.013